

NUREG/CR-1129
SAND79-1217
R7

ASSESSMENT OF POSITRON ANNIHILATION
AS A NON-DESTRUCTIVE EXAMINATION TECHNIQUE



J. A. Van Den Avyle, W. B. Jones,
W. B. Gauster, W. R. Wampler

Printed March 1980



Sandia National Laboratories

Prepared for
U. S. NUCLEAR REGULATORY COMMISSION

H003
0/1

8201280136

NOTICE

This report was prepared as an account of work sponsored by an agency of the United States Government. Neither the United States Government nor any agency thereof, or any of their employees, makes any warranty, expressed or implied, or assumes any legal liability or responsibility for any third party's use, or the results of such use, of any information, apparatus, product or process disclosed in this report, or represents that its use by such third party would not infringe privately owned rights.

The views expressed in this report are not necessarily those of the U. S. Nuclear Regulatory Commission.

NUREG/CR-1129
SAND79-1217
R7

ASSESSMENT OF POSITRON ANNIHILATION
AS A NON-DESTRUCTIVE EXAMINATION TECHNIQUE

J. A. Van Den Avyle and W. B. Jones
Mechanical Metallurgy Division 5835

W. B. Gauster
Physical Research Division 8347

W. B. Wampler
Ion-Solid Interactions Division 5111

Printed: March 1980

Sandia Laboratories
Albuquerque, New Mexico 87185
operated by
Sandia Corporation
for the
U. S. Department of Energy

Prepared for
Division of Reactor Safety Research
Office of Nuclear Regulatory Research
U. S. Nuclear Regulatory Commission
Washington, DC 20555
Under Interagency Agreement DOE 40-550-75
NRC FIN No. A-1172

ABSTRACT

Positron annihilation measurements respond sensitively to atomic-scale defects in metals. Therefore, scoping studies were initiated to evaluate the potential of the method as a non-destructive examination technique. In this program the Doppler broadening technique has been used to measure defect densities generated during plastic deformation by cold work or fatigue at room and at elevated temperatures. The primary goals have been: 1) to assess the sensitivity of the technique, 2) to correlate positron annihilation readings with observed microstructural changes in order to better understand the physical bases for these readings, and 3) to determine correlations among positron annihilation measurements and fraction of life or damage.

Positron annihilation measurements have been conducted on cold worked 316 stainless steel and pure nickel and on low cycle fatigued 316 stainless steel cycled at 293 K and at 866 K. The readings increase monotonically with damage and saturate at approximately 20% strain in cold work and at 10% of life in low and elevated temperature fatigue. In 316 stainless steel much lower sensitivity is observed for fatigue at 866 K than at 293 K.

Annealing studies on deformed samples, combined with transmission electron microscopy and microhardness results, indicate that positron annihilation is sensitive to vacancies generated by cold rolling or fatigue at room temperature. The same results indicate that positron annihilation is sensitive also to dislocations in pure nickel, but is insensitive to dislocations in 316 stainless steel. For that reason, the positron annihilation technique does not appear to be well suited to non-destructive examination of elevated temperature deformation of 316 stainless steel since excess vacancies generated by deformation above 600 K are mobile and anneal during deformation. This is corroborated by the observed low sensitivity to deformation.

A number of engineering questions on the application of positron annihilation for non-destructive examination of components and structures have been identified. While none rule out the method, considerable development work would be necessary for its implementation.

1.0 INTRODUCTION

This report describes progress in work performed as part of an ongoing contract with the Nuclear Regulatory Commission entitled "Elevated Temperature Design Assessment" (Contract DE-AC04-76-DPO0789). A primary activity in this program has been to investigate new non-destructive examination techniques which could serve to monitor damage accumulation resulting from creep and fatigue during elevated temperature service.

Current ASME design rules for nuclear structural components operating at temperatures in excess of 700 K use a "damage accumulation" approach. This method identifies segments of the creep and fatigue history, assigns life fraction values to each of these segments, and sums the life fractions to calculate a damage fraction. In this approach, when the damage fraction equals a critical value, a fracture should occur. Implicit in this concept is the assumption that the material has a memory of its past history; this analysis does not consider flaws, crack initiation and growth, or specific fracture mechanisms of creep and fatigue.

It is well known that bulk microstructural changes do occur during creep and fatigue of metals. Dislocation density can increase or decrease depending on the initial state of the metal, and these changes may alter the cyclic and creep flow stress. Precipitates can form with time at elevated temperature, with the rate of formation strongly affected by concurrent deformation. During creep deformation, internal voids can form, principally at grain boundaries, and these ultimately link to create cracks and eventual failure.

The occurrence of microstructural evolution during elevated temperature deformation suggests that this evolution might provide measurable variables which could be correlated with accumulation of "damage". If a non-destructive examination technique were developed to make these measurements, the technique, with the necessary correlations, would be a monitor of damage and would fit in the framework of current ASME design philosophy.

A new method for studying internal defect structures in metals is positron annihilation. This technique has been used successfully to measure dislocation

2.0 EXPERIMENTS

All experimental data were generated using the Doppler broadening method of positron annihilation measurements. This method, along with specimen preparation techniques and mechanical testing were detailed in a previous report (6), and only the major points will be outlined here.

Measurements were performed using a Doppler broadening apparatus, shown schematically in Figure 1, which was available from previous work. The configuration required using small disk-shaped samples approximately 0.6 cm diameter by 0.13 cm thick. These samples were sectioned from mechanical test specimens, so this particular measurement scheme was not truly non-destructive. As described later (Section 6), however, there are practical ways of making the measurements without sectioning.

Positrons were obtained from sources containing either ^{22}Na or ^{68}Ge sandwiched between the two samples. As shown in Table 1, the average depths of penetration of the positrons are small, consequently only the near-surface regions of samples contribute to the positron annihilation measurement. For the sectioned samples, this still corresponds to the interior of mechanical test specimens, provided the sectioned pieces were electropolished to remove damage caused by cutting (6). Surface preparation for non-destructive examination of structures is discussed in Section 6.

Positrons which enter a metal slow down rapidly and subsequently annihilate with electrons within about 10^{-10} s. The positrons may annihilate with electrons in the lattice, or they may become trapped at defects and annihilate with an electron associated with the defects. Ideally, the annihilation event most often produces two γ photons, each of which would have an energy of 511 keV and be emitted at 180° to each other if both the positron and electron were at rest. In fact, however, the positron is usually close to rest while the electron is not, and this causes the energies of annihilation photons to be Doppler shifted thus conserving energy. In the Doppler broadening method, an energy resolving detector is used to register photons, and the result is an energy distribution plot of counts versus energy (channel number in Figure 1). The shape of the photon energy distribution curve can be described by a

POSITRON ANNIHILATION DOPPLER BROADENING

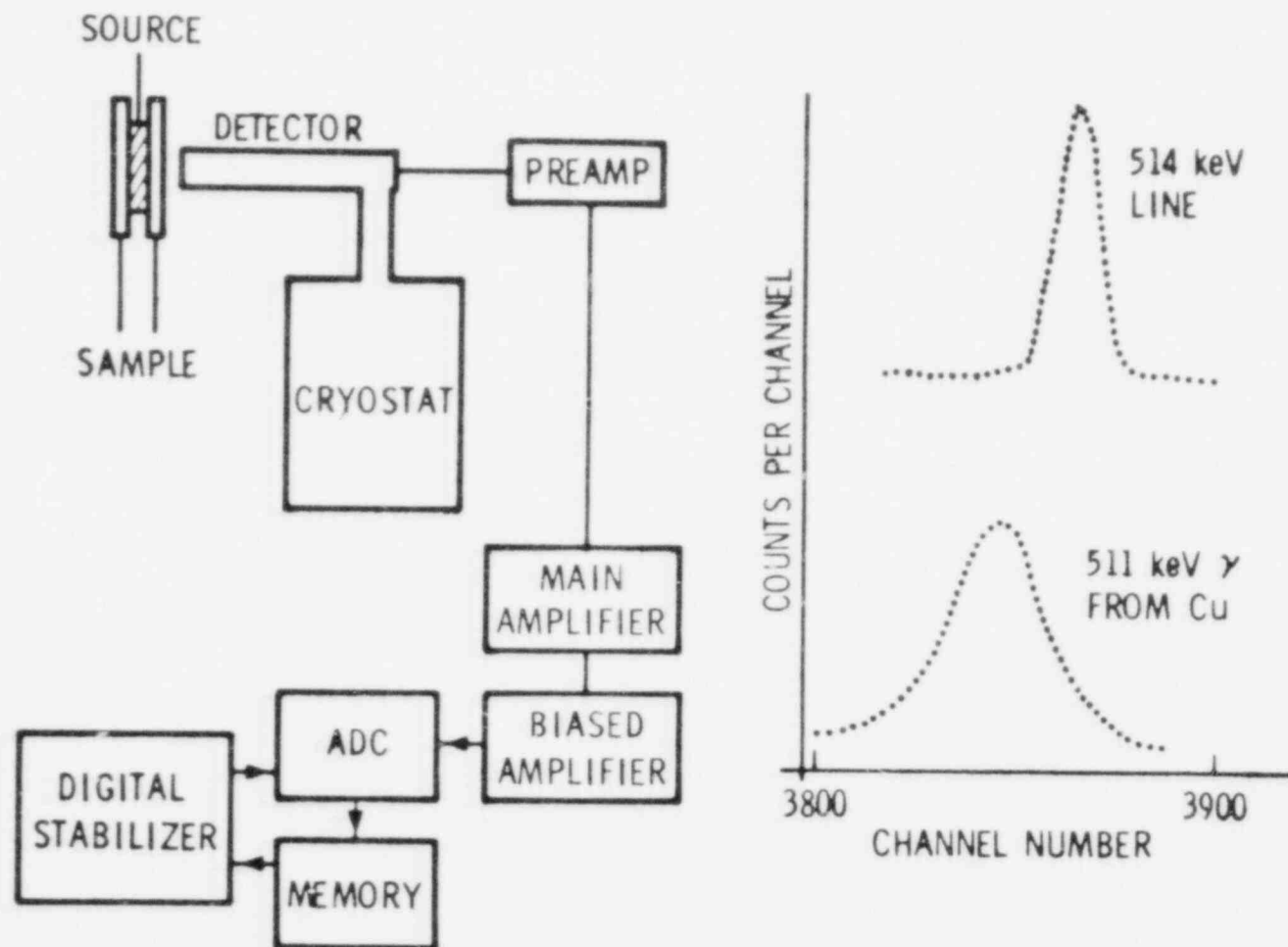


FIGURE 1. Positron annihilation Doppler-broadening spectrometer arrangement and example of data.

TABLE 1. DEPTHS OF PENETRATION OF POSITRONS IN COPPER
 (Values for Steel will be ~ 10 to 20% Higher)

<u>Source</u>	<u>e-Folding Distance</u> *	<u>Maximum Penetration</u>
²² Na	23.1 μ m = 0.0009 in	0.31 mm = 0.012 in
⁶⁸ Ge	165 μ m = 0.006 in	1.42 mm = 0.056 in

*Depth in material at which positron flux is 1/e (37%) of its value at the surface.

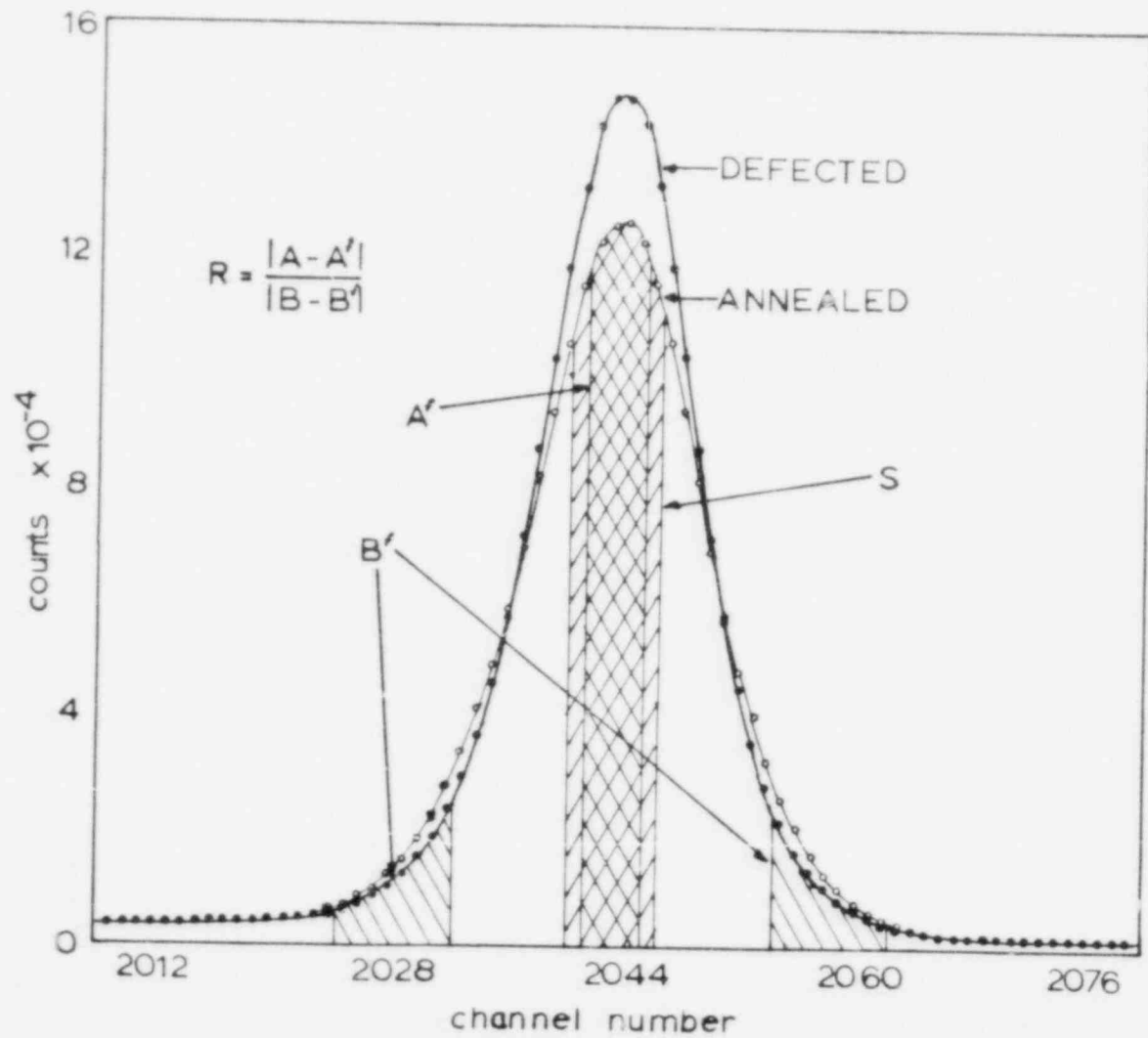


FIGURE 2. Photon energy spectra of well-annealed and defected samples with indicated channel width areas used to calculate S and R.

3.0 RESULTS

3.1 COLD WORKED NICKEL AND 316 STAINLESS STEEL

Initial scoping measurements were performed on cold rolled 316 stainless steel to assess sensitivity to varying amounts of deformation. Samples were cold worked in stages up to 75% thickness reduction. In Figure 3 the measured positron annihilation response is plotted as percentage change in lineshape parameter, relative to the well-annealed condition, versus reduction in thickness. Measurements were made on material with two starting conditions: mill-annealed "As-Received" and re-annealed (1338 K for 1 hr in vacuum). The data show an increase in lineshape parameter, reaching a saturation value at approximately 25% reduction. Data for both as-received and re-annealed 316 stainless lie along the same line. Counting statistics yield calculated error limits of approximately $\pm 2\%$ of the total measured effect.

Also plotted on Figure 3 are lineshape parameter changes for pure nickel generated by Dlubek et al. (9). Although the plotting scales have been adjusted to provide a common relative saturation level, the important point is that the behaviors of the two face centered cubic metals are nearly identical.

3.2 316 STAINLESS STEEL FATIGUE

A summary of data generated from low cycle fatigue of 316 stainless steel at both room temperature and 866 K is presented in Figure 4. The major observations which can be made are:

- 1) For a given test condition, saturation in lineshape parameter occurs within approximately 10% of life.
- 2) At 294 K, the apparent saturation value is slightly lower for the smaller strain range tests than at the higher strain range.
- 3) The ultimate saturation value for the tests at 866 K is much lower than the 294 K data at roughly equivalent strain ranges.
- 4) Tests with several combinations of hold periods show positron annihilation saturation values equivalent to non-hold period runs, even though fatigue life was reduced by a factor of four for the tensile hold case.

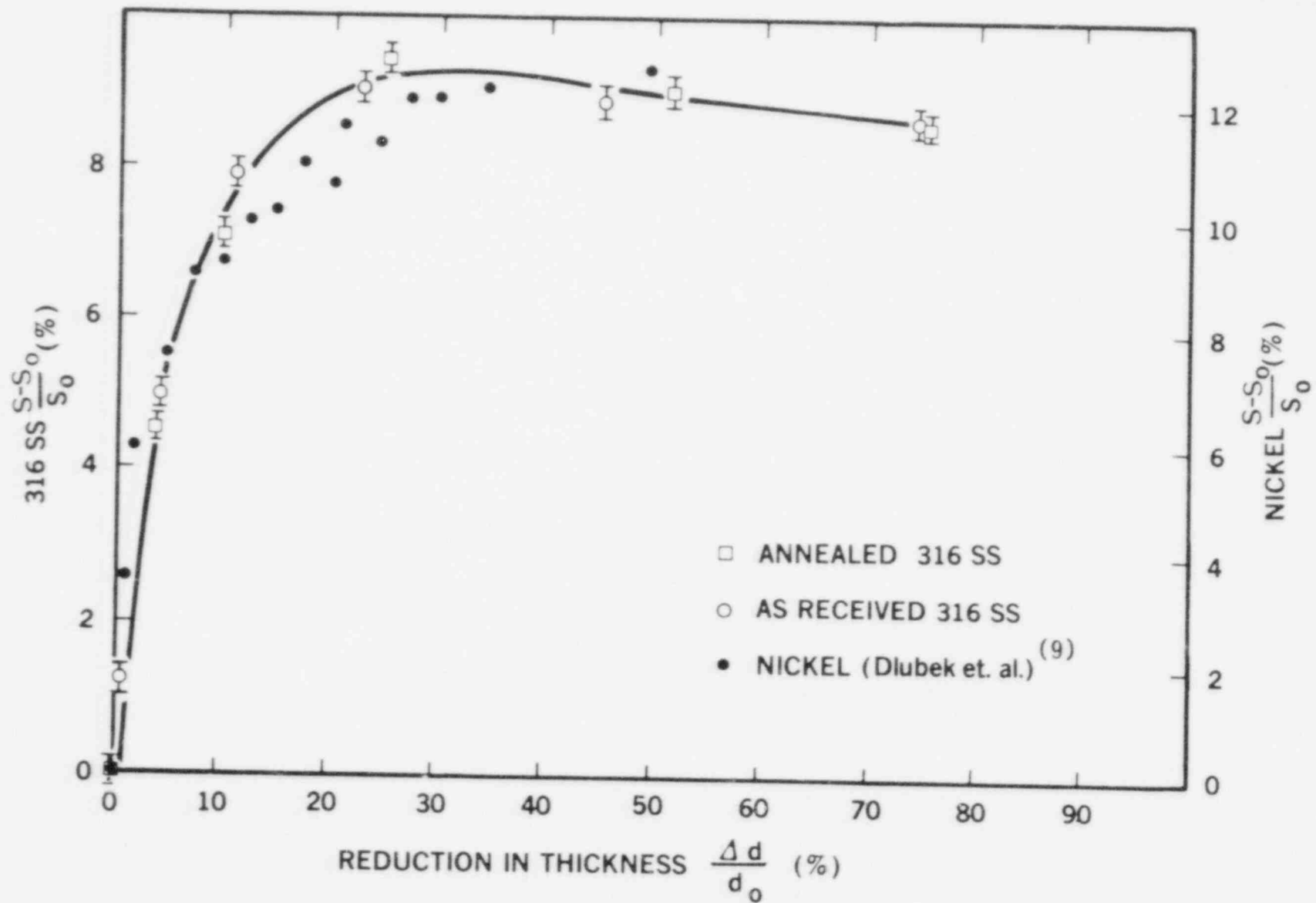


FIGURE 3. Positron annihilation response of cold worked 316 stainless steel and nickel.

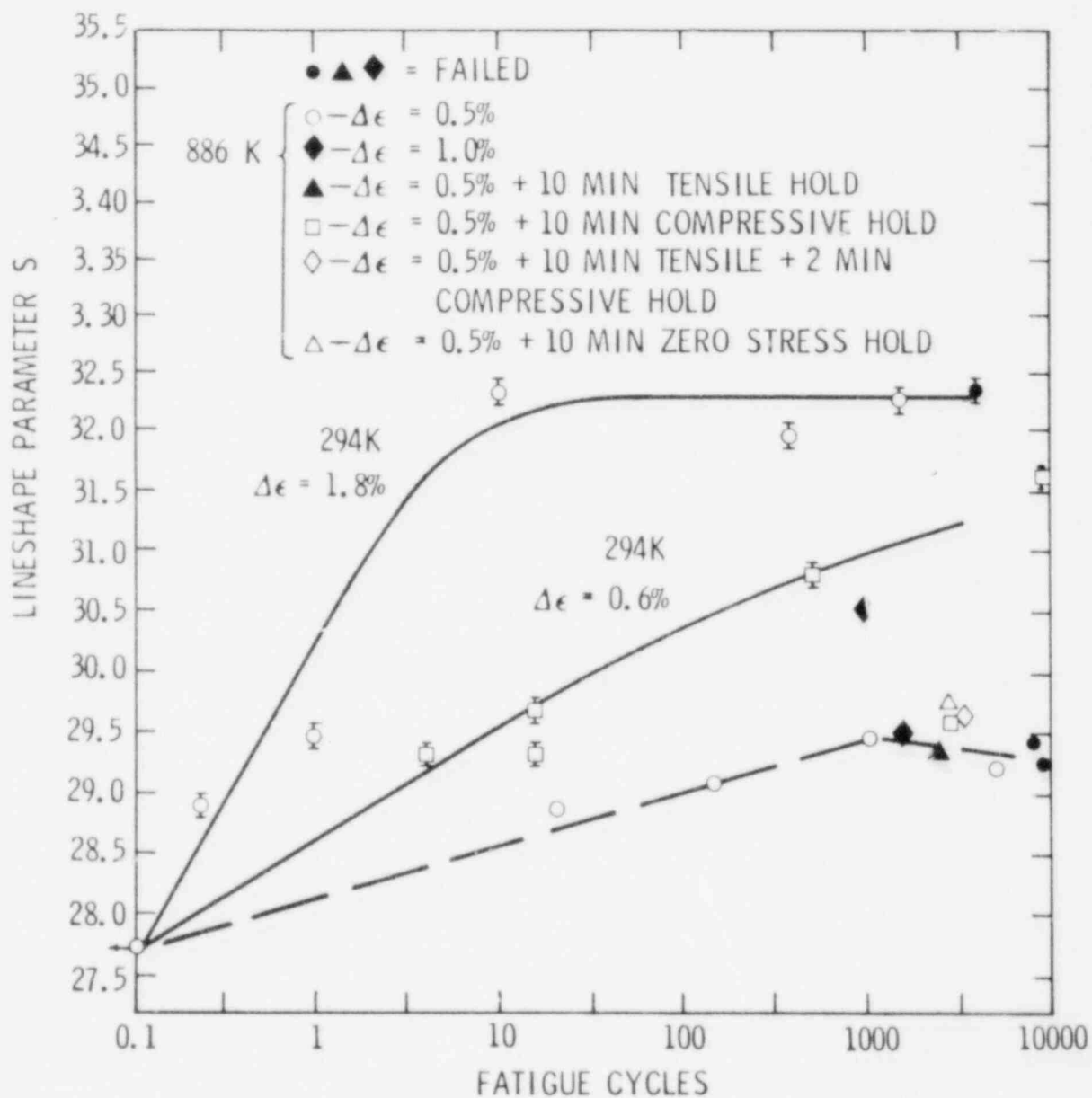


FIGURE 4. Positron annihilation response of 316 stainless steel fatigued at 293 K and 866 K.

Examinations of these fatigue specimens using transmission electron microscopy show, for each given test condition, an increase in both dislocation density and lineshape parameter with number of cycles. The micrographs in Figure 5 taken from the specimens cycled at 294 K and $\Delta\epsilon = 1.8\%$ reveal increasing dislocation densities with cycles until attainment of a saturation density. The changes observed in the positron annihilation measurements on this sample also showed saturation at about 10 cycles (see Figure 4). Further cycling produced a rearrangement of the dislocations (Figure 5) rather than any significant change in their density or the lineshape parameter.

Examination of samples from the saturation regime of each test condition in Figure 4 showed that the lineshape parameter was not a unique function of the dislocation density. For example, the lineshape parameters at saturation for the two 294 K test conditions are not greatly different, but the dislocation densities at saturation differ significantly (Figure 6a and 6b). Also, the ultimate dislocation density of the elevated temperature fatigued specimens at saturation is equal to or greater than for either of the room temperature conditions (Figure 6c), yet the saturated lineshape parameters for the elevated temperature cases are much lower. The annealing studies described in the next section indicate that these differences are due to lattice vacancies.

3.3 ANNEALING RESPONSE OF DEFORMED PURE NICKEL AND 316 STAINLESS STEEL

3.3.1 Annealing of Pure Ni

Pure Ni was selected as a model material for the annealing investigation since it has been well studied using resistivity (10,11) and calorimetry (11) techniques, and because it exhibited a response comparable to that of 316 stainless steel in cold work measurements as discussed in Section 3.1. A polycrystalline sample was cold rolled 25%, a level corresponding to positron annihilation saturation, and isochronally annealed for 30 minutes in 25 K increments from 294 K to 925 K. Lineshape parameter values measured after each annealing step are plotted as open circles in Figure 7a versus the annealing temperature. The S parameter is seen to decrease in two distinct stages, occurring at nearly the same temperatures as the annealing stages of residual

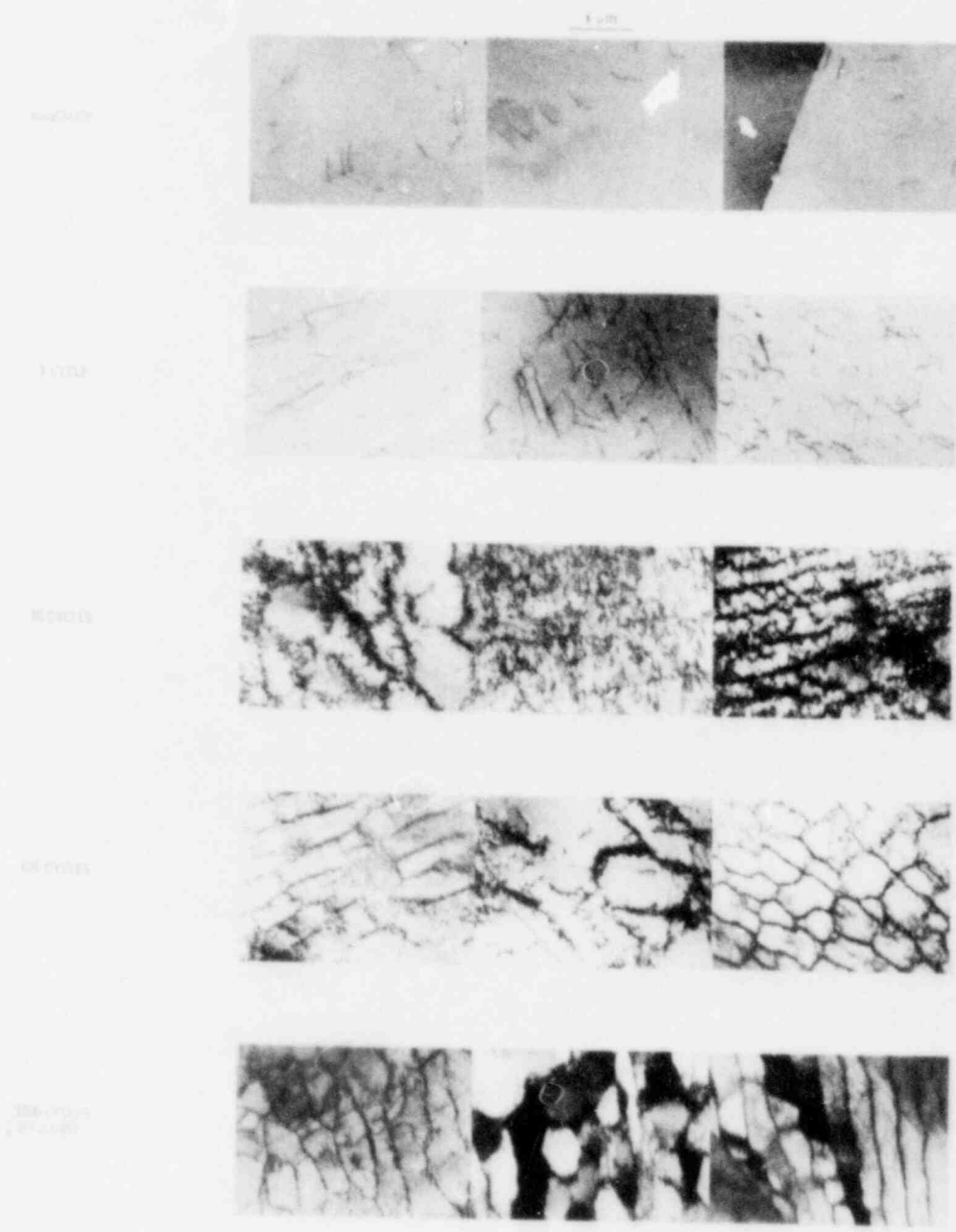
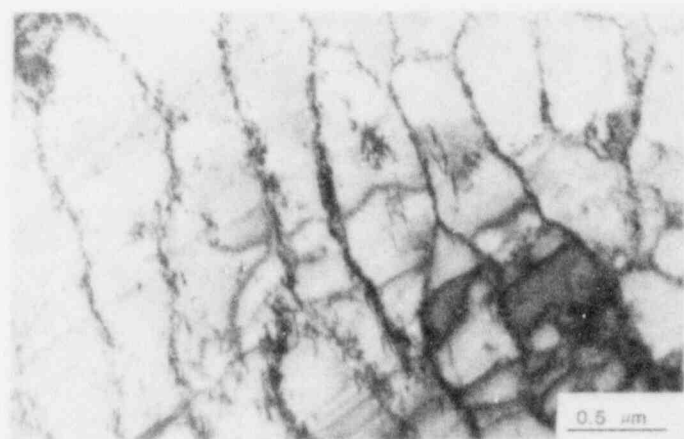


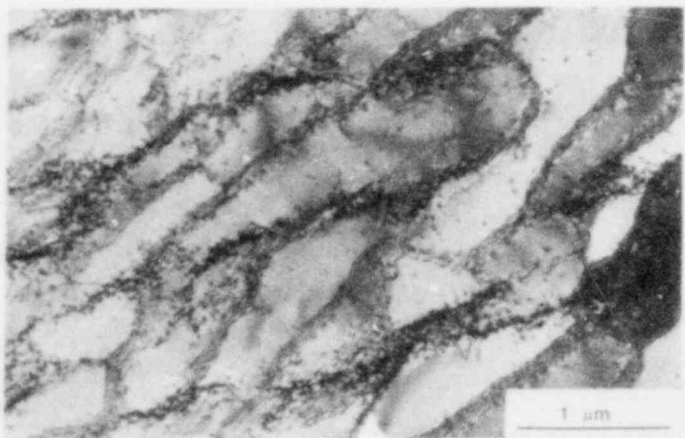
FIGURE 3. Dislocation microstructures of 316 stainless steel produced by room temperature fatigue at $\Delta\epsilon = 1.0\%$.



(a)



(b)



(c)

FIGURE 6. Microstructure of 316 stainless steel specimens fatigued to saturation of the positron annihilation lineshape parameter: a) 293 K, $\Delta\epsilon = 0.60\%$, $N = 47143$ cycles; $\bar{g} = (111)$, near $[110]$ zone; b) 293 K, $\Delta\epsilon = 1.8\%$, $N_f = 3700$ cycles; $\bar{g} = (002)$, near $[100]$ zone; c) 866 K, $\Delta\epsilon = 0.5\%$, $N_f = 10078$ cycles; near $[110]$ zone, not two beam diffraction conditions.

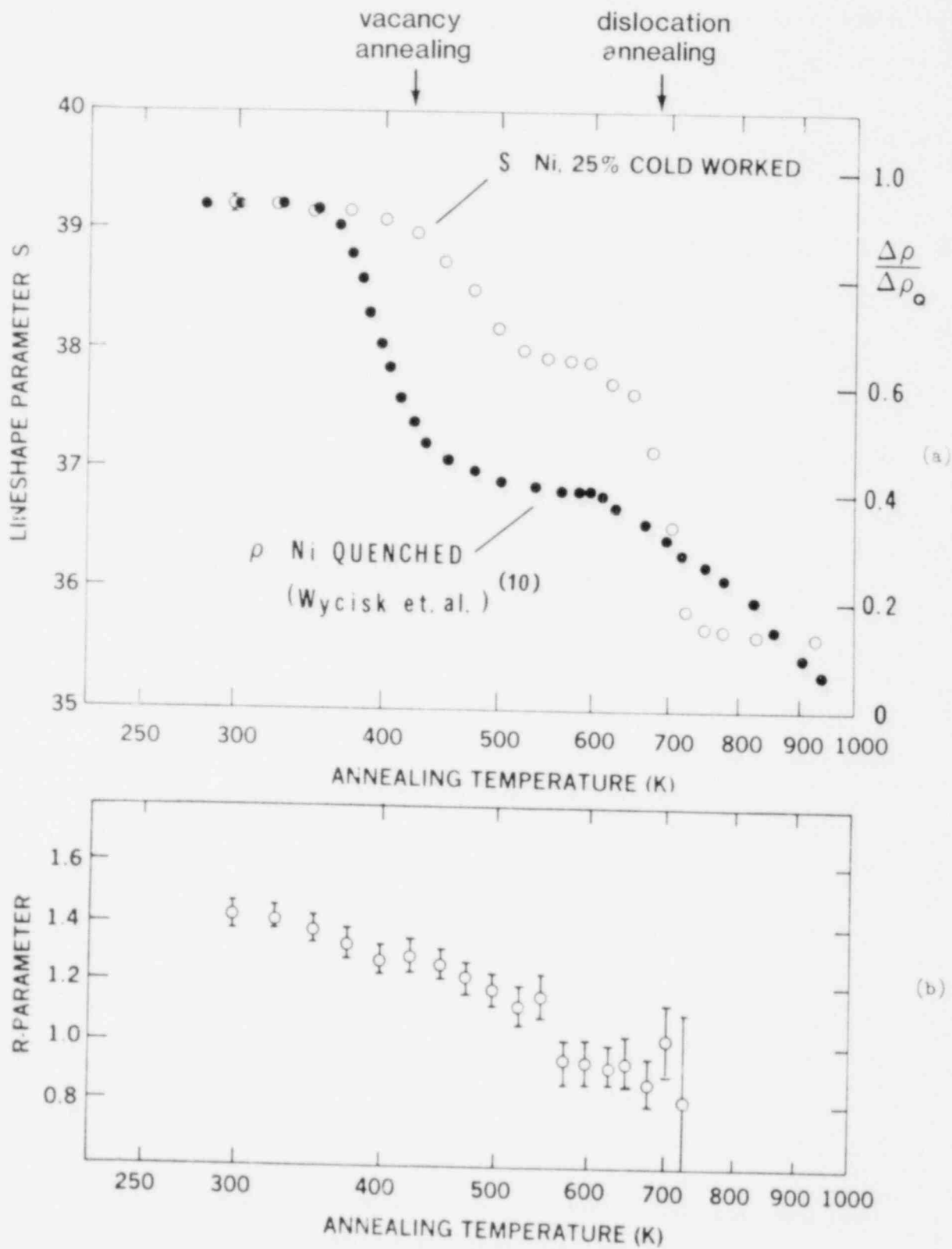


FIGURE 7. Isochronal annealing response of pure nickel: a) S-parameter measurements of cold worked nickel with resistivity data for quenched nickel by Wycisk et al. (10); b) calculated R-parameter versus annealing temperature.

resistivity (also Figure 7a) measured for quenched Ni by Wycisk and Feller-Kniepmeier (10). From this close correspondence with resistivity measurements, we conclude that the same mechanisms are operative: the first lower temperature annealing stage occurs when vacancies become mobile (recovery), and the second stage is due to the disappearance of dislocations (recrystallization). This interpretation was confirmed by transmission electron microscopy: micrographs of 25% cold worked Ni samples showed no change in the dislocation structure after annealing at 575 K (the end of the first stage) but did show a low dislocation density after annealing at 800 K. Thus the data show clearly that positrons are sensitive to dislocations in Ni and that the drop in S near 700 K is due to the disappearance of the dislocations.

The R parameter, which is another lineshape parameter mentioned in Section 2.0, is designed to have a value specific to the dominant trapping defect, but independent of defect concentration. It is calculated from the same data used to calculate S . (See References 7 and 8 for detailed discussions concerning the definition of R and relevant assumptions.) Values of R for annealing of 25% cold worked Ni are plotted in Figure 7b. Consistent with the S -parameter annealing stages, the decrease in R between 375 K and 550 K is associated with a change in the dominant type of trapping site from vacancies to dislocations; as the dislocation density decreases during the second annealing stage (550 K to 725 K) no further change in R is observed.

From these results we conclude that the positron annihilation response in cold worked Ni is due to positron trapping at vacancies alone or at both vacancies and dislocations. The response after annealing above 550 K is due to positron trapping principally at dislocations.

3.3.2 Annealing of Cold Worked 316 Stainless Steel

The results of similar annealing experiments on 316 stainless steel cold worked to 25% thickness reduction are shown in Figure 8. The decrease in S begins at a higher annealing temperature than for Ni and proceeds more gradually without resolution into two distinct stages. By 873 K, S has decreased to the value of the undeformed alloy. The R parameter remains nearly constant to 600 K and shows a slight decrease at higher temperatures; errors in the R calculation become large above 800 K since it is found by taking the ratio of differences between two pairs of nearly equal numbers.

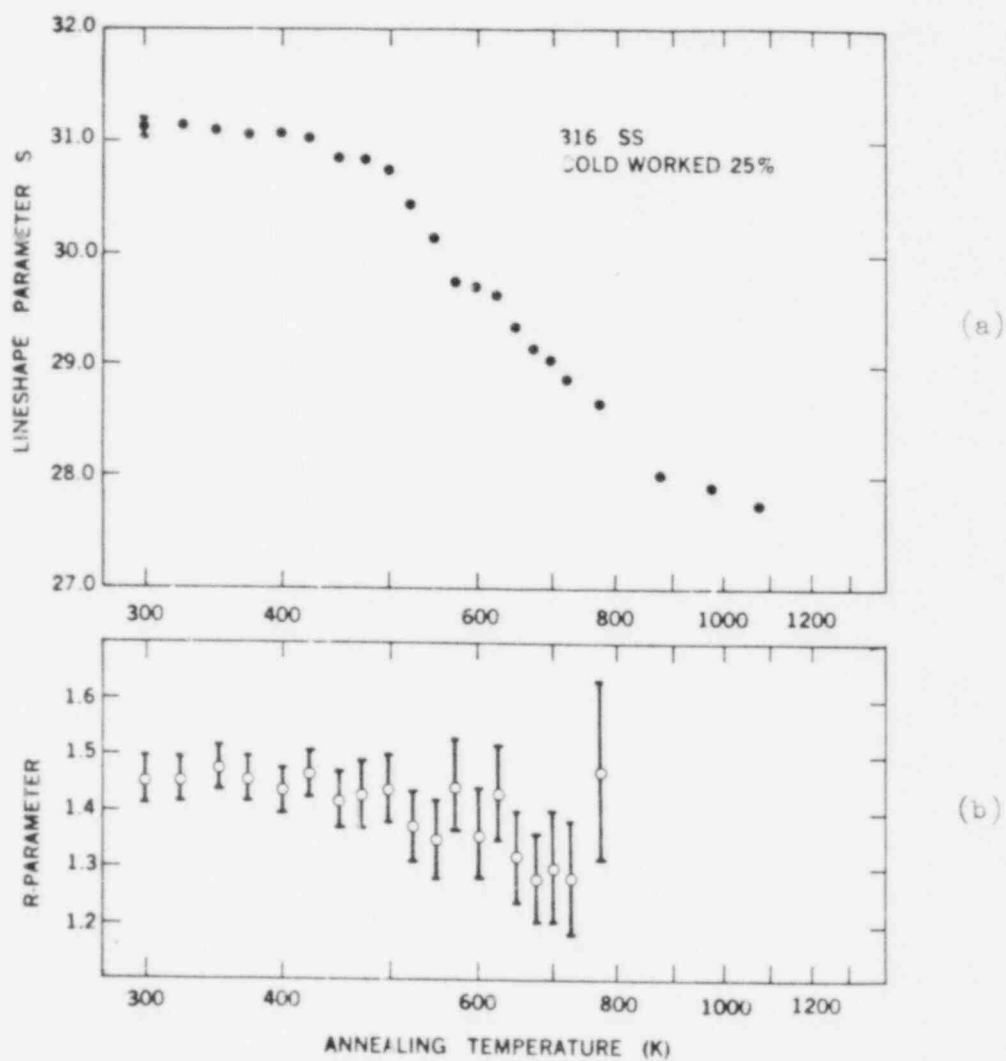


FIGURE 8. Isochronal annealing response of 25% cold worked 316 stainless steel: a) S-parameter versus annealing temperature; b) R-parameter versus annealing temperature.

To further investigate the annealing response of 316 stainless steel, microhardness isochronal annealing curves were determined. Hardness for this alloy depends primarily on the dislocation density, so a decrease in hardness after a given annealing step would imply a decrease in number of dislocations present. Microhardness values were measured at room temperature following sequential 30 minute annealing steps between 294 K and 1050 K. Data for 25% and 75% cold worked samples are given in Figure 9. The major observation to be made from these measurements is that the hardness does not decrease until annealing well in excess of 873 K. This is in contrast to the positron annihilation results of Figure 8 which show a decrease to the pre-deformation S value essentially complete by 800 K. Transmission electron microscopy observations of a 75% cold worked sample annealed to 873 K (Figure 10b) indicate a dislocation density unchanged from the as-worked state (Figure 10a) - a result consistent with the microhardness readings. Samples annealed to 1073 K have a well annealed structure (Figure 10c) and low hardness.

From this series of experiments on cold rolled 316 stainless steel, we have concluded that the positron annihilation technique applied here is insensitive to dislocations in this alloy. The decrease in S on annealing to 873 K is primarily due to annealing of vacancies or vacancy clusters.

3.4 ANNEALING RESPONSE OF FATIGUED 316 STAINLESS STEEL

The annealing response of samples taken from the saturation plateau regions of the three fatigue curves from Figure 4 are presented in Figure 11a-c. Lineshape parameter changes are expressed here as ΔS :

$$\Delta S = \frac{S - S_0}{S_1 - S_0}$$

where S is the parameter after a given annealing step, S_0 is the annealed value, and S_1 is the initial value on the $\Delta s = 1.8\%$, room temperature fatigue curve.

The annealing curves generated for the two room temperature fatigued specimens (Figure 11a and b) are very similar and exhibit the same behavior as the 25% cold rolled sample; the curves steadily decrease starting at 500 K and reach the well-annealed level at 800-900 K. In contrast, annealing of a fatigue sample cycled at

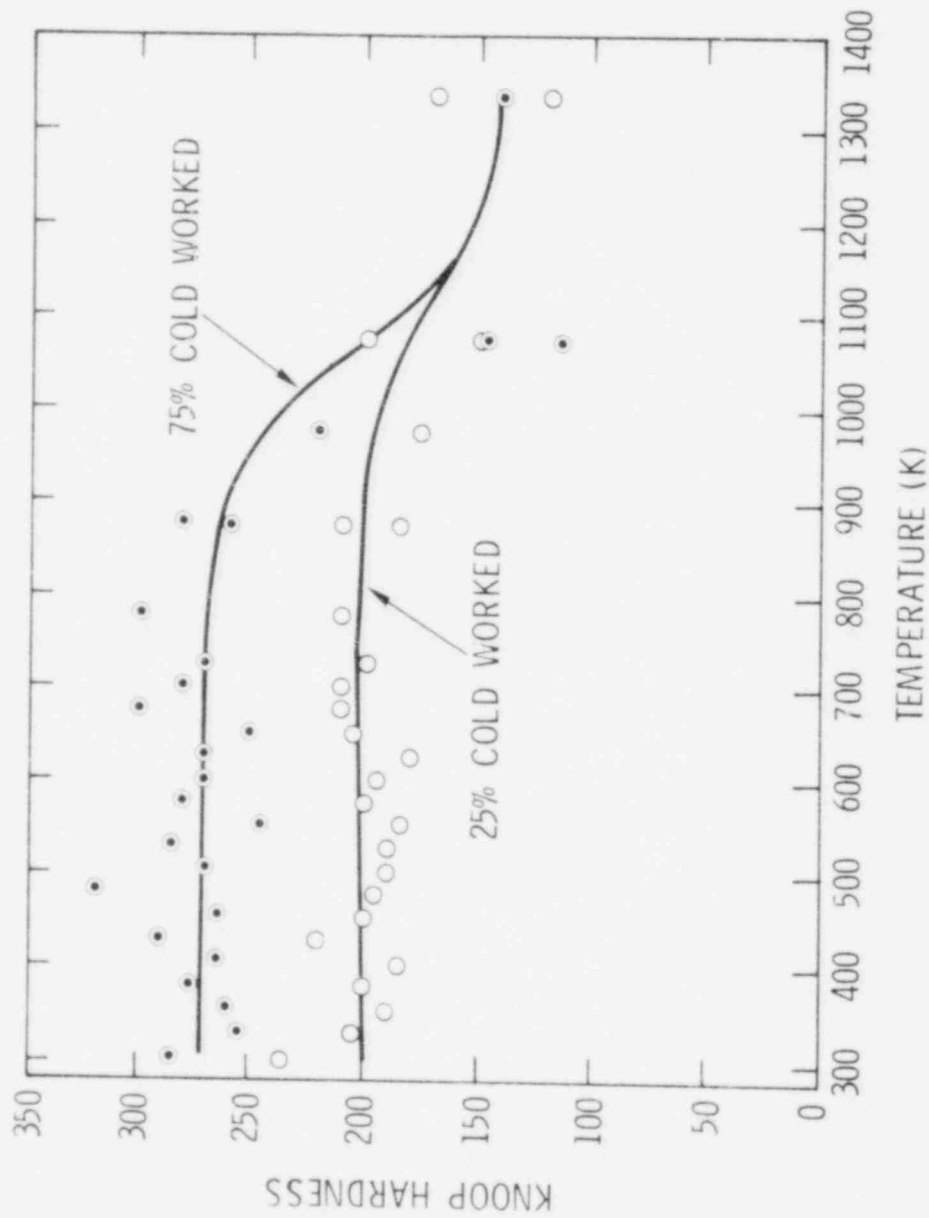
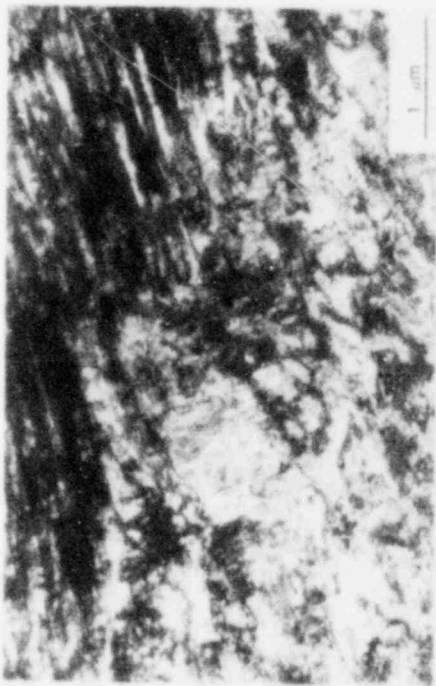


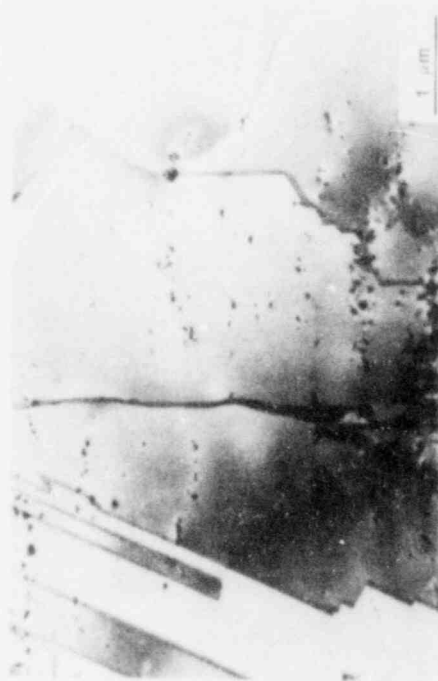
FIGURE 9. Microhardness changes produced by step-annealing cold worked 316 stainless steel.



(a)



(b)



(c)

FIGURE 10. Microstructures of 75% cold worked 316 stainless steel produced by isochronal step annealing: a) as cold rolled; b) annealed to 873 K; c) annealed to 1073 K.

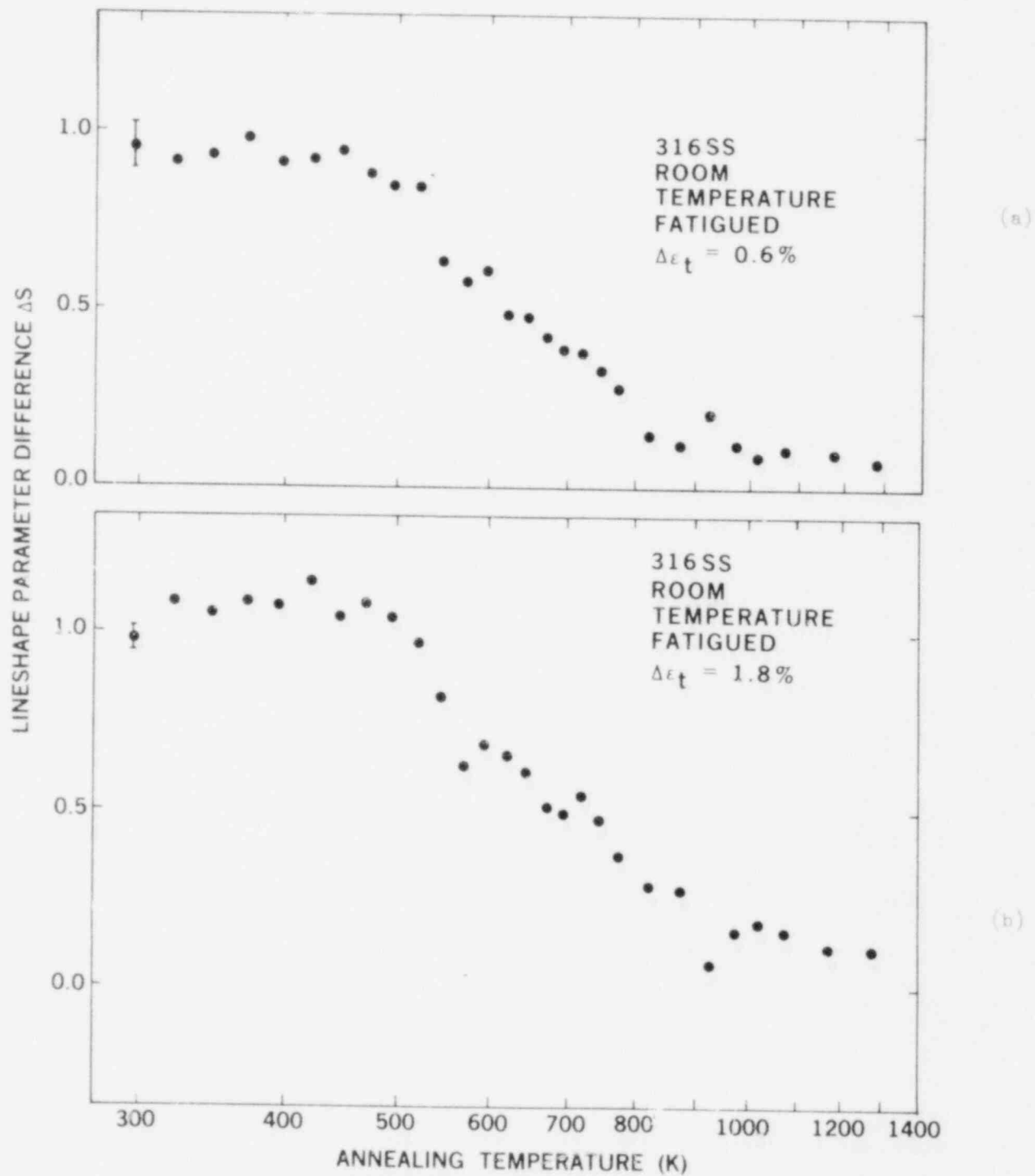
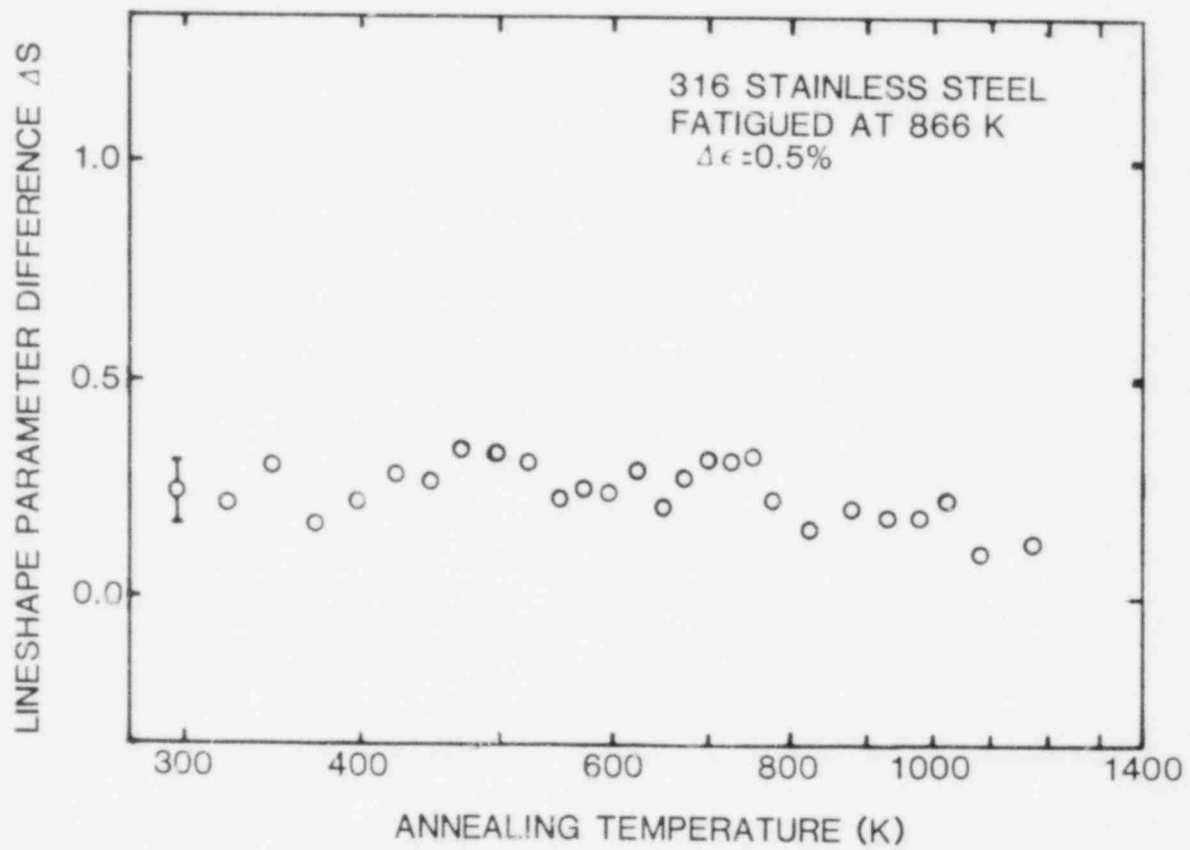


FIGURE 11. Isochronal annealing response of fatigued 316 stainless steel: a) fatigued 293 K, $\Delta\epsilon = 0.6\%$, $N_f = 47143$ cycles (prior to failure); b) fatigued 293 K, $\Delta\epsilon = 1.8\%$, $N_f = 3700$ cycles; c) fatigued 866 K, $\Delta\epsilon = 0.5\%$, $N_f = 10078$ cycles. (Lineshape parameter difference, ΔS , defined in text.)



(c)

866 K does not produce any significant decrease in ΔS (Figure 11c). This is consistent with the view that S is primarily sensitive to vacancies: in this alloy vacancies would be mobile and would diffuse to sinks during fatigue cycling at 866 K. Thus the increase in S with cycles would be small (Figure 4) and there would be few residual vacancies to anneal (Figure 11c).

3.5 DESCRIPTION OF ADDITIONAL POSITRON ANNIHILATION MEASUREMENTS

In the course of this research, several other experiments were performed which yielded negative results but which were informative.

Doppler broadening measurements were made on 316 stainless steel creep specimens tested at 866 K up to 7% creep strain. S did not change significantly after any of these test conditions. Microstructurally, the creep tests produce a small increase in dislocation density, and increases in vacancy concentration during long term testing at 866 K would be negligible. No other defects were generated in significant density to trap positrons, so the lack of change in S is not surprising.

A trial series of measurements was made using an alternate positron annihilation technique, angular correlation, which measures the deviation from a 180° path angle between the two annihilation photons. This method was described in an earlier report (6). The configuration of the angular correlation set-up is not suitable for in-service inspection, and its use here was intended primarily as a research tool since: 1) it is in principle more accurate than the Doppler broadening technique, and 2) with the existing set-up, measurements could be made on the surface of specimens without sectioning. This would allow sequential sampling of individual mechanical tests. The technique, however, requires counting times of the order of 36 hr, compared to 0.5 hr for Doppler broadening counting, using the rather low activity positron sources available here. Results of measurements on several fatigue samples showed large scatter and statistical error bars, caused by long term electronics drift during the long counting periods. In principle, there are several possible improvements which could be made; but it was decided to drop angular correlation in favor of a redesigned Doppler broadening apparatus which will allow surface measurements.

Preliminary Doppler broadening measurements have been made using a modified sample-source geometry with a remote positron source which allow measurements to be made on the surface of samples without sectioning. With the new geometry, sequential measurements can be made on individual fatigue specimens. Results so far indicate that the sensitivity and time to accumulate data are comparable to the sandwich source geometry.

4.0 DISCUSSION OF EXPERIMENTAL RESULTS

The lack of positron annihilation response to dislocations in 316 stainless steel implies either that dislocations trap positrons only weakly, or else the presence of alloying elements causes the S parameter for positrons annihilating at dislocations to be similar to the S parameter for positrons annihilating in the perfect lattice. To discriminate between the two hypotheses would require more basic research and theoretical interpretation. In any case, the ability of positron annihilation to monitor elevated temperature deformation (above 700 K) in 316 stainless steel is doubtful since vacancies generated also simultaneously anneal and the resultant observed signal is weak.

The observed increase in S for fatigue of 316 stainless steel at 866 K (Figure 4) cannot be explained by an increase in dislocation density with cycling. The positron traps which contribute to this increase in S have not been definitely established. It is possible that some residual vacancies or vacancy clusters caused by deformation remain in the sample at the end of the fatigue test. Since the specimen cools down relatively rapidly at the end of the test (~ 200 K/min), some vacancies may be "quenched" in and serve as positron traps. The data of Figure 11c, however, show no evidence of vacancy annealing. A second potential positron trap which has been observed by transmission electron microscopy (12) are small ($.02 \mu\text{m}$) carbides which precipitate heterogeneously during fatigue of this alloy at 866 K. The trapping effectiveness of these carbides have not been investigated further.

Data for pure nickel do demonstrate sensitivity to dislocations, and McKee et al. have demonstrated positron trapping at dislocations in pure copper (1). Elevated temperature deformation could probably be followed for these two pure metals. It is not known whether positron annihilation could monitor dislocation changes in any other commercially available high temperature alloy, as the understanding of alloying effects on positron trapping at dislocations is poorly developed.

The positron annihilation response to low temperature fatigue and monotonic deformation shows good sensitivity in the early stages of deformation up to 10% of life or 20% cold work. However, the readings approach a constant value after this, which would be due either to saturation in the number of defects generated or to a

saturation determined by trapping of every positron at a defect. In the latter case, the measured effect would depend on positron flux and not on defect concentration. The result is that the technique is not sensitive to the later stages of deformation. This would restrict its application to a monitor of early life or of transient overloads. It could, however, be used as a screening tool to determine whether a flaw detection non-destructive examination measurement should be performed. Also, it is possible that early life surface readings could be correlated with deformation leading to fatigue crack initiation.

The limited experiments performed here on elevated temperature samples cycled with various hold periods (Figure 4) show that positron annihilation does not correlate with reduction in life due to creep/fatigue interaction. Tests with various combinations of hold periods fall along the same curve as samples without holds. This is not unexpected given the results of electron microscopy and positron annihilation on specimens deformed by creep or fatigue alone and with creep/fatigue interaction: 1) creep alone does not provide large numbers of defects (vacancies or dislocations); 2) the only microstructural difference noted by transmission electron microscopy is an increase in numbers of small carbide precipitate in the creep/fatigue tests compared to the fatigue tests. The decrease in life due to creep/fatigue interaction is due to a more rapid fracture process, such as enhanced crack initiation and/or propagation, and positron annihilation readings are not directly related to these processes.

An additional need which has been identified here is for a defect-specific line-shape parameter, such as the R parameter, which would serve to identify the type of dominant defect. This would complement the quantitative parameter S, since S measures only total defect concentration. It would insure that measurements of concentration changes followed consistently the same type of defect. The R parameter values reported for pure Ni (Figure 7) behave as expected for a defect-specific parameter, but R values calculated for 316 stainless steel samples are ambiguous (Figure 8). Further numerical analysis needs to be performed on annihilation photon energy spectra data already collected in this program to better refine the energy channel widths used in the calculation of R (Figure 2).

5.0 MICROSTRUCTURAL EVOLUTION AS A MONITOR OF DAMAGE

The recent work in the area of bulk microstructural changes occurring during creep and fatigue has provided a good understanding of the nature and extent of these changes in tests of types 304 and 316 stainless steel (13,14). With this information, the validity of using a particular method such as positron annihilation to determine bulk microstructural evolution to predict fracture can be discussed.

The dominant microstructural change resulting from cycling, creep loading, or their combination is the rearrangement of dislocations toward a steady-state substructure characteristic of the imposed stresses and strains. Changes in dislocation density may also occur, with the density increasing during tests of annealed material or the density decreasing during tests of initially cold worked material. These are the only variations occurring during low homologous temperature deformation of single phase alloys and are still the dominant changes due to deformation of austenitic stainless steels above 600 K, even though some carbide precipitation occurs.

This substructural evolution begins with the first fatigue cycle or the first minute of a creep test and is usually complete in less than about 20% of the total specimen life (15). The steady-state dislocation density and distribution plus the progressive precipitation occurring during the test do influence the final fracture processes; however, the substructural changes occurring early in life are not directly related to the number of cycles to failure or the time to failure. In general, the bulk substructure evolves as a function of the number of cycles or time from the start of the test and reaches the steady-state condition well before any clear indication of crack initiation. Crack initiation is directly traceable back from the end of a test using crack propagation behavior, and substructure evolution is related to the start of the test; but there is no discernible relationship between the attainment of a steady-state substructure and crack initiation. This type of relationship, at best indirect, would be possible only by gaining a complete understanding of all the processes involved in creep and fatigue fracture and their interactions in each alloy system.

These conclusions are based primarily on results from transmission electron microscopy which is a good tool for observing the important microstructural changes which affect fracture processes. At best, a non-destructive examination technique which measures these variations would monitor the same changes observed in the electron microscope. If the changes observed by electron microscope cannot be directly related to fatigue or creep life results, then no microstructurally sensitive non-destructive examination technique exists which could be used directly for life prediction.

6.0 ENGINEERING APPLICATION OF POSITRON ANNIHILATION TO NON-DESTRUCTIVE EXAMINATION OF STRUCTURAL COMPONENTS

A number of potential engineering questions have been posed on the application of positron annihilation as a non-destructive examination system. These are hardware and operations problems which are independent of the positron annihilation-damage correlation question which has been discussed in Section 4.0. Here, several of these items are identified and discussed, but considerable engineering development would be needed to obtain complete answers.

6.1 POSITRON ANNIHILATION SURFACE MEASUREMENTS OF COMPONENTS

The current best estimate of a prototypic system would make Doppler broadening measurements using computer-controlled counting electronics and data processing. A coincident counting technique could be used to minimize spurious counts of background γ photons; this would use two detectors at 180° to each other and have electronics configured to trigger a count only when two γ 's from single annihilation events arrive simultaneously. Using suitable detectors and source (Section 6.2 below), counting times for a measurement would be on the order of one-half hour with reference standards used to calibrate the system. The test unit could be reasonably portable and could fit in a double electronics rack. A problem with the 180° coincident counting technique is that the geometry would not allow sampling of recessed or flat areas or components with large radii of curvature.

6.2 POSITRON SOURCES AND SOURCE PLACEMENT

A variety of isotopic positron emitters are potentially available. The major variables are the half-life of the isotope, which determines the usable life of the source, and the end-point energy of the emitted positrons, which determines their depth of penetration into the sample. A listing of several candidates is given in Table 2. The trade-off's between high and low end-point energy positrons and their effect on positron annihilation sensitivity have not been established. For practical non-destructive examination applications, it is likely that long half-life isotopes would be preferred; and high activity sources would minimize counting times. Source placement on the exterior surfaces of components is expected to be straightforward.

TABLE 2. ISOTOPES USED AS POSITRON SOURCES, WITH THEIR HALF LIVES, PRODUCTION REACTIONS, AND POSITRON END-POINT ENERGIES.

Isotope	Half-Life	Positron End-Point Energy E_{\max} (MeV)	Production Reactions
^{22}Na	2.58 yr	0.54	$^{25}\text{Mg}(p,\alpha)^{22}\text{Na}$
$^{44}\text{Ti}/^{44}\text{Sc}$	47 yr	1.47	$^{42}\text{Ca}(\alpha,2n)^{44}\text{Ti}$
^{55}Co	18.2 h	1.50	$^{58}\text{Ni}(p,\alpha)^{55}\text{Co},$ $^{56}\text{Fe}(p,2n)^{55}\text{Co}$
^{57}Ni	36.0 h	0.85	$^{56}\text{Fe}(^3\text{He},2n)^{57}\text{Ni}$
^{58}Co	71.3 days	0.48	$^{58}\text{Ni}(n,p)^{58}\text{Co},$ $^{55}\text{Mn}(\alpha,n)^{58}\text{Co}$
^{64}Cu	12.9 h	0.65	$^{63}\text{Cu}(n,\nu)^{64}\text{Cu}$
^{65}Zn	245 days	0.33	$^{64}\text{Zn}(n,\nu)^{65}\text{Zn}$
$^{68}\text{Ge}/^{68}\text{Ga}$	275 days	1.88	$^{66}\text{Zn}(\alpha,2n)^{68}\text{Ge}$
^{69}Ge	40 h	1.22	$^{69}\text{Ga}(d,2n)^{69}\text{Ge}$
^{90}Nb	14.7 h	1.50	$^{90}\text{Zr}(p,n)^{90}\text{Nb},$ $^{90}\text{Zr}(d,2n)^{90}\text{Nb}$

For measurements on inside surfaces such as piping, however, the positron source must be located on the inside. This would be a difficult mechanical movement problem for complex structural geometries. Annihilation γ 's generated from inside surfaces could be detected through several inches of steel.

6.3 SURFACE PREPARATION AND AREAS OF INSPECTION

Since the maximum penetration depth of positrons is limited (of the order of 0.3-1.4 mm), any surface deformed region, oxidation, or coatings would need to be removed in order to take measurements of material representative of the bulk. The preparation method used in this study, electropolishing, could be performed on selected areas of interest. These regions would then have to be protected from subsequent surface damage during the life of the plant.

Because of the need for surface preparation, it is unlikely that the entire surface area of a component could be scanned. It would be most practical to select critical locations for inspection which analysis predicts as having high potential for damage.

6.4 INITIAL STATE OF THE ALLOY

It is certain that different areas of components would have varying initial levels of vacancy or dislocation defect concentrations. This would require baseline measurements for each location to be monitored, and these could be compared to data for well-annealed samples of the same alloy to assess the initial state. Any residual cold work performed on the components or structure as a result of fitting or joining operations would show up. It is possible that regions with significant cold work would give high initial positron annihilation readings close to saturation values for S, thereby confusing interpretation of established damage correlations.

7.0 CONCLUSIONS

- 7.1 In 316 stainless steel and nickel cold worked or fatigued at room temperature, positron annihilation measurements primarily show sensitivity to vacancies generated during deformation. In nickel the vacancies anneal out by 550 K, leaving dislocations in the microstructure; for pure nickel positron annihilation is sensitive to dislocation density.
- 7.2 In 316 stainless steel positrons are insensitive to dislocation density. This was demonstrated by comparing positron annihilation readings, transmission electron microscopy, and microhardness measurements.
- 7.3 For 316 stainless steel positron annihilation lineshape parameter increases monotonically with damage and saturates at approximately 20% strain in cold work and at 10% of life in low and elevated temperature fatigue. Thus positron annihilation readings are best suited to monitoring the early stages of deformation. Potentially these early values of surface damage could be correlated to fatigue crack initiation criteria.
- 7.4 In 316 stainless steel much lower sensitivity is observed for elevated temperature fatigue than for room temperature fatigue. Thus positron annihilation does not appear to be well suited as a non-destructive monitor of 316 stainless steel at elevated temperature. This results from the low sensitivity to dislocations and the mobility of vacancies generated by deformation at temperatures above 600 K (620°F).
- 7.5 Since not all changes in bulk microstructure are related to the fracture processes, observations of these changes by positron annihilation, electron microscopy, or other techniques may only provide indirect correlations to the extent of damage. These correlations would need to be established for each alloy of interest.
- 7.6 In addition to the problem of damage correlations, a number of engineering questions on the application of positron annihilation as a non-destructive examination technique for components and structures have been identified. While none rule out the technique, considerable development work would be necessary.

ACKNOWLEDGEMENT

We thank J. C. Banks for assistance with the positron annihilation measurements and C. R. Hills for performing the transmission electron microscopy.

REFERENCES

1. B. T. A. McKee, S. Saimoto, A. T. Stewart, and M. J. Stott, *Can. J. Phys.* 52, 759 (1974).
2. S. Berko and J. C. Erakine, *Phys. Rev. Lett.* 19, 307 (1967).
3. J. C. Grosskreutz and W. E. Millett, *Phys. Lett.* 28A, 621 (1969).
4. C. F. Coleman and A. E. Hughes, in *Research Techniques in Nondestructive Testing*, R. S. Sharpe, ed., (Academic Press, New York and London, 1977) Vol. 3.
5. C. F. Coleman, F. A. Smith, and A. E. Hughes, UKAEA Harwell Report AERE-R8951 (1966).
6. W. B. Gauster, W. R. Wampler, W. B. Jones, and J. A. Van Den Avyle, Sandia Laboratories Report SAND-77-1570, U. S. Nuclear Regulatory Commission Report NUREG/CR-0118 (1978).
7. W. Triftshäuser, *Phys. Rev. B* 12, 4634 (1975).
8. S. Manti and W. Triftshäuser, *Phys. Rev. B* 17, 1645 (1978).
9. G. Dlubek, D. Brümmer, and E. Hensel, *Phys. Stat. Sol. (a)* 34, 737 (1976).
10. W. Wycisk and M. Feller-Kniepmeier, *J. of Nuc. Mats.*, 69 & 70, 616 (1978).
11. L. M. Clarebrough, M. E. Hargreaves, and M. H. Loretto, "Changes in Internal Energy Associated with Recovery and Recrystallization," *Recovery and Recrystallization of Metals*, AIME Symposium, Feb. 20-21, 1962, Gordon and Breach, 1963.
12. Present authors, research to be published.
13. H. Nahn, J. Motteff, and D. R. Biercks, *Acta Met.* 25, 107-116 (1977).
14. K. D. Challenger and J. Motteff, *Met. Trans.*, 4, 749-755 (1973).

DISTRIBUTION:

U. S. Nuclear Regulatory Commission
(310 copies for R7)
Division of Document Control
Distribution Services Branch
7920 Norfolk Avenue
Bethesda, MD 20014

U. S. Nuclear Regulatory Commission (54)
Division of Reactor Safety Research
Office of Nuclear Regulatory Research
Washington, D. C. 20555
Attn: C. N. Kelber, Assistant Director,
Advanced Reactor Safety Research
R. T. Curtis, Chief
Analytical Advanced Reactor Safety Research, ARSR
M. Silberberg, Chief
Experimental Fast Reactor Safety
R. W. Wright (50)
Experimental Fast Reactor Safety

U. S. Department of Energy
Office of Nuclear Safety Coordination
Washington, D. C. 20545
Attn: R. W. Barber

U. S. Department of Energy (2)
Albuquerque Operations Office
P. O. Box 5400
Albuquerque, NM 87185
Attn: J. R. Roeder, Director
Operational Safety Division
D. K. Nowlin, Director
Special Programs Division
For: C. B. Quinn
D. Plymale

University of Michigan
Nuclear Engineering Department
Ann Arbor, MI 48104

General Electric Corporation
310 De Guigne Drive
Sunnyvale, CA 94086
Attn: Manager, Dynamics and Safety

W. E. Nyer
P. O. Box 1845
Idaho Falls, ID 83401

Projekt Schneller Brueter (4)
Kernforschungszentrum Karlsruhe GMBH
Postfach 3640
D75 Karlsruhe
West Germany
Attn: Dr. Kessler (2)
Dr. Heusener (2)

Distribution (Cont'd):

Institut de Protection et de Surete Nucleaire (3)
CEN Fontenay-aux-Roses
B. P. 6
92260 Fontenay-aux-Roses
France
Attn: M. Tanguy
M. Schmitt
M. Cogne

Safety Studies Laboratory (3)
Commissariat a L'Energie Atomique
Centre d'Etudes Nucleaires de Cadarache
B. P. 1, 13115 Saint-Paul-les-Durance
Bouches-Du-Rhone
France
Attn: M. Bailly
M. Meyer Heine
M. Penet

Centre d'Etudes Nucleaires de Grenoble
B. P. 85 - Centre de Tri
38401 Grenoble, Cedex
France
Attn: M. Costa

H. J. Teague (3)
UKAEA
Safety and Reliability Directorate
Wigshaw Lane
Culcheth
Warrington, WA3 4NE
England

R. G. Bellamy
Reactor Fuels Group
AERE Harwell
Oxfordshire, OX11 0RA
England

R. G. Tyrer, Head
Reactor Development Division
UKAEA - Atomic Energy Establishment
Winfrith, Dorchester
Dorset
England

Joint Research Centre (2)
Ispra Establishment
21020 Ispra (Varese)
Italy
Attn: R. Klersy
H. Holtbecker

Distribution (Cont'd):

Power Reactor & Nuclear Fuel
Development Corporation (PNC) (2)
Fast Breeder Reactor Development Project (FBR)
9-13, 1-Chome, Akasaka
Minato-Ku, Tokyo
Japan
Attn: Dr. Mochizuki
Dr. Watanabe

1100 C. D. Broyles
Attn: G. E. Hansche, 1120
G. L. Ogle, 1125
H. F. Viney, 1130
J. H. Davis, 1136

1537 N. B. Keltner
Attn: B. W. Acton
T. Y. Chu

1550 F. W. Neilson
Attn: O. J. Burchett, 1552
J. H. Gieske, 1552

2150 T. L. Workman

3434 B. W. Yates

4000 A. Narath

4231 J. H. Renken
Attn: J. A. Halbleib
P. J. McDaniel
J. E. Morel

4400 A. W. Snyder

4410 D. J. McCloskey

4420 J. V. Walker

4422 R. L. Coats

4422 J. E. Gronager

4422 G. W. Mitchell

4422 D. A. Powers

4422 J. B. Rivard

4422 D. W. Varela

4423 J. E. Powell

4423 G. L. Cano

4423 A. C. Marshall

4423 J. G. Kelly

4423 D. A. McArthur

4423 K. O. Reil

4423 H. L. Scott

4423 K. T. Stalker

4423 W. H. Sullivan

4423 S. A. Wright

4424 P. S. Pickard

4424 J. T. Hitchcock

4424 D. H. Worledge

4425 W. J. Camp

4425 B. W. Ostensen

4425 D. C. Williams

4425 M. F. Young

4425 R. J. Lipinski

4425 W. M. Breitung

4441 M. L. Corradini

4442 W. A. Von Riesenmann (25)

4450 J. A. Reuscher

4450A L. D. Posey

Distribution (Cont'd):

4451 T. R. Schmidt
4723 D. O. Lee
5110 R. L. Schwoebel
5111 S. T. Picraux
5111 W. R. Wampler (5)
5500 O. F. Jones
5530 W. Herrmann
5534 D. A. Benson
5534 J. E. Smardyk
5800 R. S. Claassen
5820 R. E. Whan
5822 N. E. Brown
5830 M. J. Davis
5831 N. J. Magnani
5835 C. H. Karnes
5835 W. B. Jones (4)
5835 J. A. Van Den Avyle (4)
5836 J. L. Ledman
5846 E. K. Beauchamp
5846 R. A. Sallach
8347 W. B. Gauster (5)
8766 E. A. Aas
3141 T. L. Werner (5)
3151 W. L. Garner (3)
For: DCE/TIC (Unlimited Release)
3154-3 R. P. Campbell (25)
For: NRC Distribution to NTIS

